Global Change Biology

Global Change Biology (2017) **23**, 94–107, doi: 10.1111/gcb.13369

Predicting the effects of climate change on population connectivity and genetic diversity of an imperiled freshwater mussel, *Cumberlandia monodonta* (Bivalvia: Margaritiferidae), in riverine systems

KENTARO INOUE[1] and DAVID J. BERG[2]

[1]*Department of Biology, Miami University, 700 East High Street, Oxford, OH 45056, USA,* [2]*Department of Biology, Miami University, 1601 University Boulevard, Hamilton, OH 45011, USA*

Abstract

In the face of global climate change, organisms may respond to temperature increases by shifting their ranges poleward or to higher altitudes. However, the direction of range shifts in riverine systems is less clear. Because rivers are dendritic networks, there is only one dispersal route from any given location to another. Thus, range shifts are only possible if branches are connected by suitable habitat, and stream-dwelling organisms can disperse through these branches. We used *Cumberlandia monodonta* (Bivalvia: Unionoida: Margaritiferidae) as a model species to investigate the effects of climate change on population connectivity because a majority of contemporary populations are panmictic. We combined ecological niche models (ENMs) with population genetic simulations to investigate the effects of climate change on population connectivity and genetic diversity of *C. monodonta*. The ENMs were constructed using bioclimatic and landscape data to project shifts in suitable habitat under future climate scenarios. We then used forward-time simulations to project potential changes in genetic diversity and population connectivity based on these range shifts. ENM results under current conditions indicated long stretches of highly suitable habitat in rivers where *C. monodonta* persists; populations in the upper Mississippi River remain connected by suitable habitat that does not impede gene flow. Future climate scenarios projected northward and headwater-ward range contraction and drastic declines in habitat suitability for most extant populations throughout the Mississippi River Basin. Simulations indicated that climate change would greatly reduce genetic diversity and connectivity across populations. Results suggest that a single, large population of *C. monodonta* will become further fragmented into smaller populations, each of which will be isolated and begin to differentiate genetically. Because *C. monodonta* is a widely distributed species and purely aquatic, our results suggest that persistence and connectivity of stream-dwelling organisms will be significantly altered in response to future climate change.

Keywords: dendritic network, ecological niche modeling, forward-time population genetic simulation, range shift, species distribution modeling, spectaclecase

Received 28 September 2015 and accepted 16 May 2016

Introduction

Over the last 100 years, mean global temperature has increased by 0.85 °C due to human-induced climate change, which is predicted to continue into the future (IPCC, 2013). Such rapid changes in global climatic regimes impact ecological processes in aquatic and terrestrial ecosystems. Given that most species tolerate short-term variability in climate through phenotypic plasticity, when species encounter changes in local climatic conditions they often respond by adjusting their phenology and physiology to match new climatic patterns (Walther *et al*., 2002). However, if a species' distributional range reflects its adaptive capability, the species will need to shift the range poleward or to higher altitude when climate warms (Hampe & Petit, 2005; Jump & Penuelas, 2005). Range shifts associated with climate change have been predicted and observed in plant and animal species worldwide (Parmesan & Yohe, 2003; Chen *et al*., 2011); such range shifts vary among individual species depending on habitat specificity and dispersal capability (Chen *et al*., 2011).

In terrestrial systems, spatially heterogeneous landscapes often have a lattice-like architecture, where patches of suitable habitat are connected by multiple dispersal paths (Urban & Keitt, 2001). Range shifts in response to climate change, therefore, depend on intrinsic dispersal capabilities of species and habitat

Correspondence: Kentaro Inoue, Aquatic Systems Biology Unit, Department of Ecology and Ecosystem Management, Technical University of Munich, Mühlenweg 22, 85354 Freising, Germany, tel. +89 8161 71 3947, fax +89 8161 71 3477, e-mail: inouek@miamioh.edu

connectivity across the landscape. Riverine systems, on the other hand, have a hierarchical dendritic structure, where physical flows often dictate distance and directionality of dispersal (Campbell Grant *et al*., 2007; Altermatt, 2013; Peterson *et al*., 2013). In a dendritic network, the dispersal route is a single path from any given location to another. In general, connectivity of riverine systems is predicted to be greater along mainstems relative to headwaters because mainstems allow movement of species among branches (Fagan, 2002; Peterson *et al*., 2013). Thus, range shifts are expected only if all branches are fully or temporarily connected with suitable habitats and stream-dwelling organisms are capable of dispersing through branches and mainstems. Despite this theoretical work, few empirical studies have demonstrated range shifts in response to climate change in dendritic networks (e.g., Booth *et al*., 2011).

Given current rates of anthropogenically driven environmental and climate change, many researchers have focused on projecting the species-level impacts of these changes. Recently, evidence has emerged linking genetic variation and patterns of environmental and climatic change (Geffen *et al*., 2004; Habel *et al*., 2011; Row *et al*., 2014; Sexton *et al*., 2014). These studies have found that changes in climatic patterns would potentially alter population genetic structure. In riverine systems, a few studies have focused on integrating dendritic landscape structure into spatial patterns of genetic variation and gene flow of aquatic taxa (Hughes *et al*., 2009; Alp *et al*., 2012). However, while such studies have demonstrated associations between population genetic structure and dendritic landscape structure, principal mechanisms relating genetic-climate interactions with range shifts in riverine systems have not been fully articulated (Heino *et al*., 2009). Riverine ecosystems comprise a wide variety of habitat types and contain high species richness. Because both habitat diversity and species diversity are vulnerable to anthropogenic disturbances (Dudgeon *et al*., 2006; Vörösmarty *et al*., 2010), it is important to understand how human-induced changes affect ecological processes in riverine systems.

Here, we investigated how changes in future climate might alter distributions and population connectivity using a wide-ranging freshwater mussel, *Cumberlandia monodonta*, as a model. Until the early 20th Century, this species was distributed throughout the Mississippi River system of the USA, including the mainstems of the Mississippi, Ohio, and Tennessee rivers, and 41 tributaries (Butler, 2002). Currently, however, the species sporadically occurs in a few locally abundant populations scattered across approximately 20 streams within the historic range, covering a great range in latitude (>10°; Fig. 1; USFWS, 2012). In 2012, relatively large populations were discovered in the Ouachita River, Arkansas, and the Green River, Kentucky (USFWS, 2014). This species generally inhabits firm mud under slab boulders or bedrock shelves in large rivers with slow to swift current (USFWS, 2014); for example, we found large numbers of mussels within stone structures used for training navigation channels in the Osage River, Missouri (personal observation). As with most freshwater mussels, *C. monodonta* possesses a complex life cycle in which larvae (glochidia) are obligate parasites of vertebrate hosts. Although numerous host-suitability trials have been conducted, the host species is/are still unknown (USFWS, 2012). A previous study reconstructing the phylogeography of *C. monodonta* revealed that the species occupied at least two glacial refugia during the mid-Pleistocene, and that populations from these refugia became admixed and spread across the current species range during the Holocene (Inoue *et al*., 2014). Based on genetic analyses, populations in tributaries of the upper Mississippi River (from the headwaters to the confluence with the Ohio River) form a panmictic population, while the Ouachita River population in the lower Mississippi basin is genetically distinct and isolated from the panmictic population. These populations are considered to be separate evolutionarily significant units. Because poleward and/or higher altitude (upstream, in the case of riverine systems) range shifts are expected in response to climate warming, current populations of *C. monodonta* will likely be further fragmented if climate change reduces habitat connectivity and prevents this species from shifting its distribution poleward or toward headwaters.

In this study, we assessed population structure of *C. monodonta* using data from a previous study (Inoue *et al*., 2014) supplemented with additional populations (Table S1) and then investigated the effects of future climate change on distributional shifts in suitable habitats and population genetic connectivity. We performed both ecological and genetic simulations to accomplish these aims. We created an ecological niche model (ENM) based on current climatic and landscape conditions to predict suitable habitat across the range where *C. monodonta* persists and projected this model based on near-future climate scenarios to examine future changes in suitable habitat and therefore species distribution. We then used a forward-time genetic simulation to project potential changes in genetic diversity and population connectivity under these future climate scenarios. If future climate scenarios show shifts in the distribution of suitable habitats poleward or toward headwaters, we predict that habitat fragmentation due to increased stretches of unsuitable habitat would restrict gene flow and thus create genetically isolated populations from the panmictic population. Because *C. monodonta* is a widely distributed species and purely

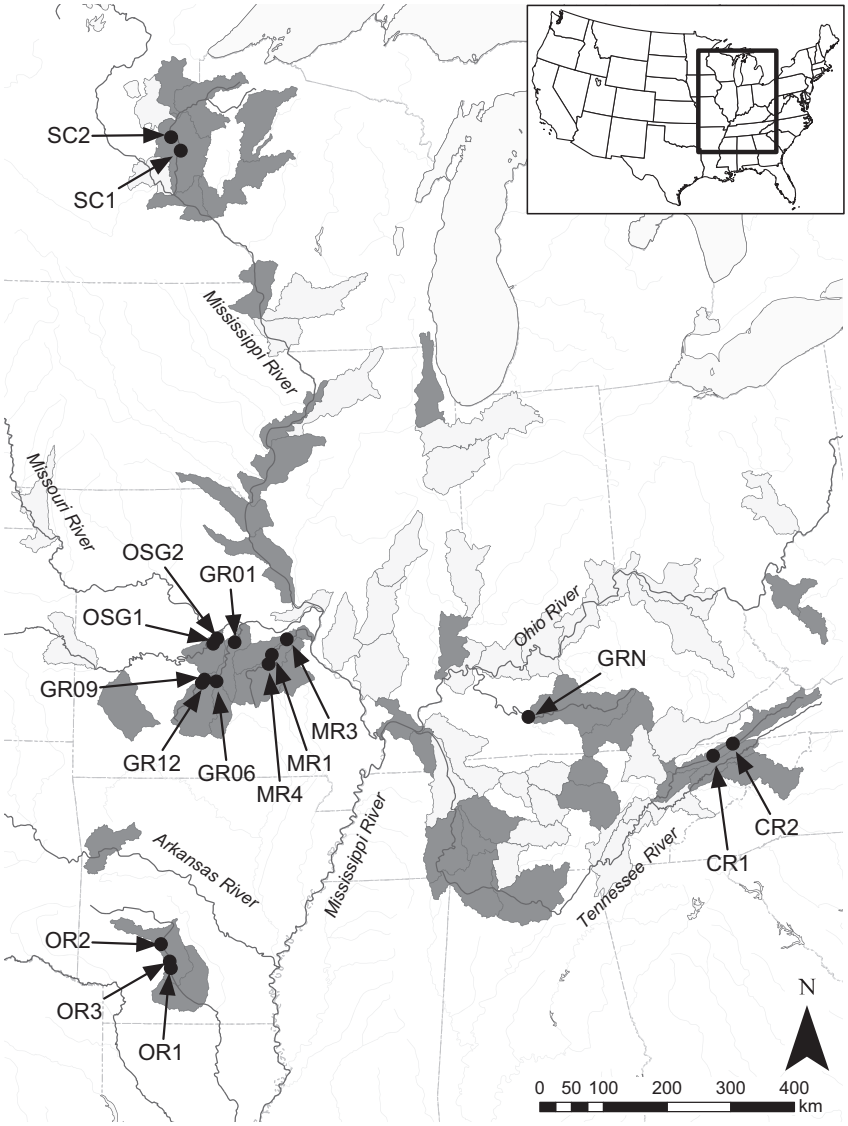

Fig. 1 Map of the central United States indicating sites where *Cumberlandia monodonta* was sampled (black dots). See Table S1 for sampled rivers and sample size at each site. Shaded watersheds represent current (dark gray) and historic (light gray plus dark gray) distributions of *C. monodonta* obtained from NatureServe (http://explorer.natureserve.org; accessed June 25, 2015).

aquatic, our results will help to identify potential changes in persistence and connectivity of stream-dwelling organisms in response to future climate change.

Materials and methods

Sampling, genetic data collection, and analyses of population genetic diversity

We used a total of 416 individuals of *C. monodonta* from 17 localities representing seven rivers in the Mississippi River Basin (Table S1 and Fig. 1). These included 119 previously collected individuals from five localities (Inoue *et al.*, 2014). The new samples were collected from 12 localities in the seven rivers using snorkeling, SCUBA, and tactile methods. Our collections represented sample sizes between 20 and 37 individuals per locality from at least two locations in each river, except only six individuals were collected from one of the sites in the Ouachita River (OR2), and only one location from the Green River was sampled (Table S1). Sampled rivers extend across four biogeographic provinces (Haag, 2009): Tennessee-Cumberland (Clinch River sites), Upper Mississippi (Gasconade, Meramec, Osage, and St. Croix rivers), Ohioan (Green River), and Mississippi Embayment (Ouachita River). All rivers, except the Ouachita, are tributaries of the upper Mississippi River. Nondestructive samples were collected from foot and mantle tissues by rubbing mucus and epidermal cells using buccal swabs (Epicentre Biotechnologies, Madison, WI, USA). Mussels were returned to the river bottom; samples were preserved in 95% ethanol and stored at −20 °C. Total genomic

DNA was extracted from swab samples using the ArchivePure DNA Cell/Tissue Kit (5 Prime, Gaithersburg, MD, USA). Extracted DNA was diluted to 10 ng μL^{-1} and used as a template in polymerase chain reactions (PCR) that amplified the mtDNA cytochrome oxidase I (COI) locus and 16 microsatellite loci (Inoue *et al*., 2011, 2014). Procedures and conditions for PCR, sequencing, fragment analyses, and postsequencing/postfragment analyses followed those in Inoue *et al*. (2014).

We estimated population genetic indices from mtDNA sequences using DNASP v5.10 (Librado & Rozas, 2009). We calculated number of haplotypes (H), mean number of basepair differences (K), and mean nucleotide diversity (π) for each locality. Because sample sizes at each locality differed, we used rarefaction to estimate the number of haplotypes (H_R) after correcting for sample-size bias. We built a haplotype network using HAPLOVIEWER (available at http://www.cibiv.at/~greg/haploviewer) after constructing a consensus parsimony tree using PHYLIP v3.695 (Felsenstein, 2005).

For microsatellite loci, we conducted exact tests for pairwise linkage disequilibrium and deviation from Hardy–Weinberg expectation (HWE) using GENEPOP v4.0.10 (Rousset, 2008) for each locality. We estimated population genetic indices (mean number of alleles per locus, N_A; and observed and expected heterozygosities, H_O and H_E) for each locality using GENALEX v6.3 (Peakall & Smouse, 2006). Additionally, we used rarefaction to correct mean allelic richness (rarefied number of alleles per locus; A_R) and mean number of private alleles per locus (N_{RP}) using ADZE v1.0 (Szpiech *et al*., 2008). We set standardized sample size to 20 and excluded one Ouachita River population (OR2) due to small sample size.

Population genetic structure

We examined partitioning of genetic variation among localities by performing an analysis of molecular variation (AMOVA) using HIERFSTAT v0.04-10 (Goudet, 2005) in R v3.0.2 (R Core Team, 2015). We partitioned genetic variation into four hierarchical levels: (i) total genetic variation among provinces (F_{PT}), (ii) genetic variation among rivers within province (F_{RP}), (iii) genetic variation among localities within river (F_{SR}), and (iv) total genetic variation among localities (F_{ST}). Statistical significance of the deviation of each F from 0 was estimated using 1000 permutations for each partition. We then estimated two indices of genetic differentiation among localities: pairwise F_{ST} using GENALEX and Jost's D_{EST} (Jost, 2008) in DEMETICS v0.8-7 (Gerlach *et al*., 2010) using R. We tested for statistical significance of deviation from 0 using 9999 permutations for pairwise F_{ST} comparisons and using 100 bootstraps for pairwise D_{EST} comparisons. We used only the microsatellite dataset for AMOVA and genetic differentiation indices.

Using STRUCTURE v2.3.4 (Pritchard *et al*., 2000), we evaluated population genetic structure of *C. monodonta* without *a priori* assignment of individuals to populations. We used the admixture model and allowed for correlated allele frequencies to account for ancestral admixture in the dataset. We ran STRUCTURE with a burn-in period of 500 000 Markov chain Monte Carlo (MCMC) generations followed by 200 000 iterations for $k = 1$ through 10 with 10 replicates for each k. We evaluated the log-likelihood [lnP(k)] for each k and estimated Δk using STRUCTURE HARVESTER (Earl & vonHoldt, 2012) to determine the most likely number of distinct clusters. We averaged each individual's admixture proportions over the 10 replicates for the best k using CLUMPP (Jakobsson & Rosenberg, 2007) and then produced graphical display results using DISTRUCT (Rosenberg, 2004).

Projecting the effects of climate change on suitable habitat

To predict suitable habitat for *C. monodonta* in the present and future throughout the Mississippi River Basin, we developed ENMs employing the maximum entropy algorithm implemented in MAXENT v.3.3.3 (Phillips *et al*., 2006). To capture the climatic optima of *C. monodonta*, we used geo-referenced occurrence points generated in this study, obtained from other recent field surveys, and obtained from museum records over the last 50 years (Table S2). These points represent the present-day distribution of *C. monodonta* in the Mississippi River Basin. Given that occurrence data often show strong spatial bias in sampling efforts, we used SDMTOOLBOX v1.0b (Brown, 2014) to reduce spatial autocorrelation in the occurrence data by selecting one record within a 5-km radius (Phillips *et al*., 2009; Kramer-Schadt *et al*., 2013). Furthermore, given the sporadic distribution of *C. monodonta* in the Mississippi River Basin, it is ecologically realistic to sample background points from the known occurrence area (Elith *et al*., 2011). Thus, we created a layer from the Gaussian kernel density of sampling locations (i.e., a bias layer) with a bandwidth of 50 km to control for background sampling efforts. We set our modeling area to include a 1-km buffer around ≥ third-order streams in the Mississippi River Basin. We initially obtained 19 bioclimatic layers and an altitude layer from WorldClim (http://www.worldclim.org; Hijmans *et al*., 2005) and two hydrological layers from the USGS National Map (http://nationalmap.gov/small_scale) and HydroSHEDS (http://hydrosheds.cr.usgs.gov; Table S3). Bioclimatic layers were estimated based on 'current conditions' (interpolations of observed data from 1950 to 2000) and four future climate scenarios (low and high greenhouse gas concentrations in 2050, averages from 2041 to 2060; and in 2070, averages from 2051 to 2080; IPCC 5th Assessment). We used two representative concentration pathways (RCPs) for low and high greenhouse gas concentration scenarios (RCP2.6 and RCP8.5, respectively). The hydrological layers include Strahler stream order and flow accumulation to create measurements of the relative sizes of rivers. We used ARCGIS v10.2 (ESRI, Inc.) and SDMTOOLBOX to produce a base-map (i.e., a 1-km buffer around streams of the Mississippi River Basin), and environmental layers with the same map projection and resolution (1 km^2). Using SDMTOOLBOX, we identified seven uncorrelated layers (Pearson correlation coefficient <0.6; see Table S3) to predict suitable habitat for *C. monodonta*.

Using MAXENT, we built ENMs based on current bioclimatic and hydrological layers, and then projected current ENMs under four future climate scenarios to predict future suitable habitats where *C. monodonta* might persist. We used the ten-fold cross-validation method to replicate models. We then

evaluated the current ENM results using the area under the curve (AUC) of the receiver operating characteristics curve (ROC). The AUC ranges from 0.5 (random accuracy) to 1.0 (perfect discrimination).

We estimated proportional changes in suitability scores for each of the occurrence points over time. Furthermore, we estimated distributional changes under the two greenhouse gas concentration scenarios. We first created binary predictions of suitable or unsuitable habitat by classifying as 'suitable' any cell with suitability values greater than or equal to the lowest value associated with any one of the occurrence points (Pearson *et al*., 2007). We used SDMTOOLBOX to estimate the distributional changes between two consecutive ENMs (i.e., ENMs of current and 2050, and ENMs of 2050 and 2070) and then calculated areas of range expansion, contraction, and no change in the species' distribution under future climate scenarios.

Projection of the effects of climate change on genetic variation and connectivity

We used the spatially explicit, individual-based landscape genetic program CDPOP v1.2.19 (Landguth & Cushman, 2010) to assess how future changes in stream connectivity might influence population genetic structure and genetic diversity of the extant populations of *C. monodonta*. CDPOP implements stochastic processes to simulate genotype frequencies through time as a function of individual-based reproduction, mortality, and dispersal on a continuous resistance surface. We considered that individual dispersal in the stream network is a function of stream connectivity through suitable habitats. Dispersal resistance matrices typically have required expert knowledge on the weighting of habitat heterogeneity to represent relevant friction values for calculation of least-cost paths (Brown, 2014). Recently, inverted ENMs have been used to create a resistance surface (i.e., a friction layer), which is a more objective alternative to the use of expert knowledge. Thus, we converted the ENM layers to friction layers in SDMTOOLBOX by simply inverting the suitability scores and calculated a stream resistance matrix for each pair of populations through stream branches based on the friction layers using Python scripts for ARCGIS described in Etherington (2011). Using this method, a path through highly suitable habitat is converted to a path of low dispersal cost. Because individuals in the upper Mississippi River belong to a currently panmictic population and there was no signature of isolation by river distance (Inoue *et al*., 2014), we considered that glochidia were able to be freely dispersed by hosts within this region. Thus, we used the maximum stream resistance value within the panmictic region as a dispersal threshold in CDPOP simulations.

We simulated three models associated with future climatic scenarios: (i) stream resistance is constant through time (no-climate-change model), (ii) stream resistance changes under the low greenhouse gas concentration scenario (RCP2.6 model), and (iii) stream resistance changes under the high greenhouse gas concentration scenario (RCP8.5 model). We applied the current stream resistance matrix for the no-climate-change model throughout the simulation. For the RCP2.6 and RCP8.5 models, we first applied the current stream resistance matrix for the first 49 years, and then applied future stream resistance matrices derived from the 2050 ENMs and the 2070 ENMs at the 50th and 70th years, respectively.

CDPOP requires a series of demographic parameters (e.g., reproductive modes and age-specific mortality rates). We assumed average sexual maturity at 10 years; equal sex ratio at birth; maximum age of reproduction as 56 years; and average fecundity of five million glochidia per spawning (Baird, 2000; USFWS, 2012, 2014). Although this species may produce two broods per year (Gordon & Smith, 1990), a more-recent study reported no evidence of biannual reproduction (Baird, 2000), and thus, we assume *C. monodonta* spawns once a year. We calculated age-specific mortality rates estimated from a static life table (adult mortality rate at 5%; Baird, 2000). Information for early life stages (e.g., glochidial and juvenile stages) is often limited. In our case, we do not have information for a transformation rate from glochidia to settled juvenile for *C. monodonta*. Thus, we used the known rate for *Quadrula fragosa* (Kjos *et al*., 1998) to estimate a mortality rate during metamorphosis. Furthermore, because it is not practical to use such a large number of individual glochidia in the simulation, we used the number of first-year juveniles per female as an estimate of fecundity, calculated from number of glochidia per female multiplied by a mortality rate during metamorphosis estimated from *Q. fragosa* (Kjos *et al*., 1998), and the mortality rate between year 0 and year 1 estimated from a static life table (Baird, 2000). Thus, we set fecundity (i.e., average number of first-year juveniles per female) at 0.453, with individual fecundities drawn from a Poisson distribution. We assumed that mating occurs completely within local populations because adult mussels are incapable of dispersing long distances (USFWS, 2012).

We used empirical microsatellite data for the simulations, after excluding individuals with missing genotypes and the OR2 population due to small initial population size. Because varied population sizes can influence the outcome (Hall & Beissinger, 2014; Landguth & Schwartz, 2014), we added hypothetical individuals and made up each population to 50 individuals. Prior to the simulations, we ran short burn-in simulations (30 years) to assign genotypes for the hypothetical individuals based on empirical allele frequencies. After the burn-in period, we had a total of 800 individuals from 16 populations that contained a total of 374 alleles over 16 loci. We aimed to simulate long-term evolutionary potential rather than short-term conservation management. Thus, we ran each simulation for 1000 years, or approximately 40 generations, with 10 Monte Carlo replications, to capture trajectories of genetic diversity and population differentiation over time. We note that because long-term future climate models are not available, our future trajectories represent conservative estimates, where climatic conditions stabilize 80 years into the future. Through this simulation, we attempted to understand the relationships between climate change and genetic trajectories of organisms with long generation times, such as *C. monodonta*. We estimated changes in population genetic structure by comparing simulated D_{EST} with the empirical estimate of D_{EST}. For each model at every year, we estimated two genetic

diversity indices within the populations over 10 replicates: total number of alleles over 16 loci and mean H_E.

Results

Population genetic diversity

Estimates of within-population variation at the COI and microsatellite loci were obtained for 17 populations from seven rivers. We recovered a total of 62 haplotypes from 412 COI sequences (Table S1); these were submitted to GenBank (accession numbers: KX255862–KX256156). Overall mean number of basepair differences was 4.05 bp, and nucleotide diversity was 0.0065. We observed similar genetic diversity in all populations, except those from the Ouachita River, which had consistently low numbers of haplotypes, numbers of base pair differences, and nucleotide diversity. As with previous results (Inoue *et al.*, 2014), we observed two haplotype lineages in our samples (Fig. S1). A majority of individuals (66.7–99.6% of individuals within a population; Table S1) were from Lineage 1 in all populations, except those from the Ouachita River; all individuals from the Ouachita populations possessed Lineage 2 haplotypes (Fig. S1), which were not shared with populations from other rivers.

Microsatellite analyses showed no evidence of linkage disequilibrium and some deviations from HWE (15% of all population-by-locus pairs) after sequential Bonferroni correction. However, these did not show any pattern across populations or loci (they were scattered among 14 populations and 10 loci; none of these loci showed departures from HWE for all populations, nor did departures from HWE reflected a consistent excess or deficiency of heterozygotes at specific loci or within individual populations). Furthermore, removing four loci which showed departures from HWE in more than 30% of populations did not significantly change later analyses (data not shown). Thus, we included all loci in further analyses. The number of alleles per locus ranged from five to 66 (for a total of 382 different alleles over 16 loci). The mean allelic richness across the 16 loci ranged from 6.37 in OR1 to 9.34 in CR1 (Table S1). The mean observed heterozygosity ranged from 0.63 in GR12 to 0.83 in GR1, and the mean expected heterozygosity ranged from 0.68 in OR2 to 0.85 in MR1. After rarefaction, there were no alleles unique to individual populations ($N_{RP} < 0$; Table S1), indicating that all alleles were shared by at least two populations.

Population genetic structure

Results of AMOVA showed significant population genetic structure in *C. monodonta* (Table S4). Genetic variation was less among localities within river ($F_{SR} = 0.003$, $P = 0.008$; Table S4) and among rivers within province ($F_{RP} = 0.001$, $P = 0.012$); higher genetic variation was found among individual localities ($F_{ST} = 0.038$, $P = 0.001$) and among provinces ($F_{PT} = 0.033$, $P = 0.001$). These results indicate little genetic differentiation among localities within the same river or province. A majority of pairwise comparisons of F_{ST} and D_{EST} were significantly greater than 0; however, ranges of these indices were small ($F_{ST} = 0$–0.097; $D_{EST} = 0.010$–0.518; Table S5). Furthermore, all high values of F_{ST} and D_{EST} ($F_{ST} = 0.057$–0.097, $D_{EST} = 0.346$–0.518) were found when comparing the Ouachita populations with those from other rivers.

Cumberlandia monodonta showed evidence of significant range-wide population genetic structure. The STRUCTURE analysis indicated differentiation between a cluster of the Ouachita populations and a cluster of all the other populations at $k = 2$ [$\Delta k = 303.6$, lnP (k) = −31453.0; Figs 2 and S2]. We found no evidence of admixture between the two clusters, and we did not recover further differentiation within clusters.

Projection of the effects of climate change on suitable habitat

All models had high AUC values (>0.85), indicating overall adequate performance. The climatic and hydrological variables that most influenced prediction of

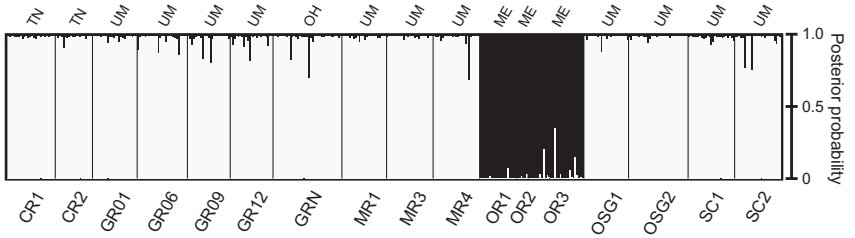

Fig. 2 Stacked bar plots obtained from STRUCTURE, assigning individuals into $k = 2$ clusters; clusters were divided by the Ouachita populations (dark gray) and the remainder of populations (light gray). Top labels are biogeographic provinces identified by Haag (2009): Tennessee-Cumberland (TN), Upper Mississippi (UM), Ohioan (OH), and Mississippi Embayment (ME). Bottom labels are *a priori* population assignments.

suitable habitat were precipitation during the driest month (51.2%) and flow accumulation (20.8%), followed by maximum temperature during the warmest month (14.4%) and mean diurnal range (8.5%). Intermediate levels of precipitation during the driest month, maximum temperature during the warmest month, and mean diurnal range were positively associated with habitat suitability scores, while flow accumulation was negatively correlated with suitability scores. The average suitability score of the occurrence points was 0.614 (SE = 0.027); scores ranged from 0.267 to 0.826. To create a binary classification of suitable and unsuitable habitats, we used the lowest suitability score for an occurrence point as the lower limit for 'suitable' habitat (0.267; Fig. 3). In addition to rivers with current and historical records of *C. monodonta* (Figs 3 and S3; USFWS, 2012, 2014), the ENMs detected potential suitable habitat in the upper White River (Arkansas), the Red River (the border of Arkansas and Oklahoma), and tributaries of the lower Mississippi River in Mississippi; no occurrences have been recorded from these. Populations in tributaries of the upper Mississippi River were connected by areas of high suitability scores, potentially allowing high gene flow among populations and

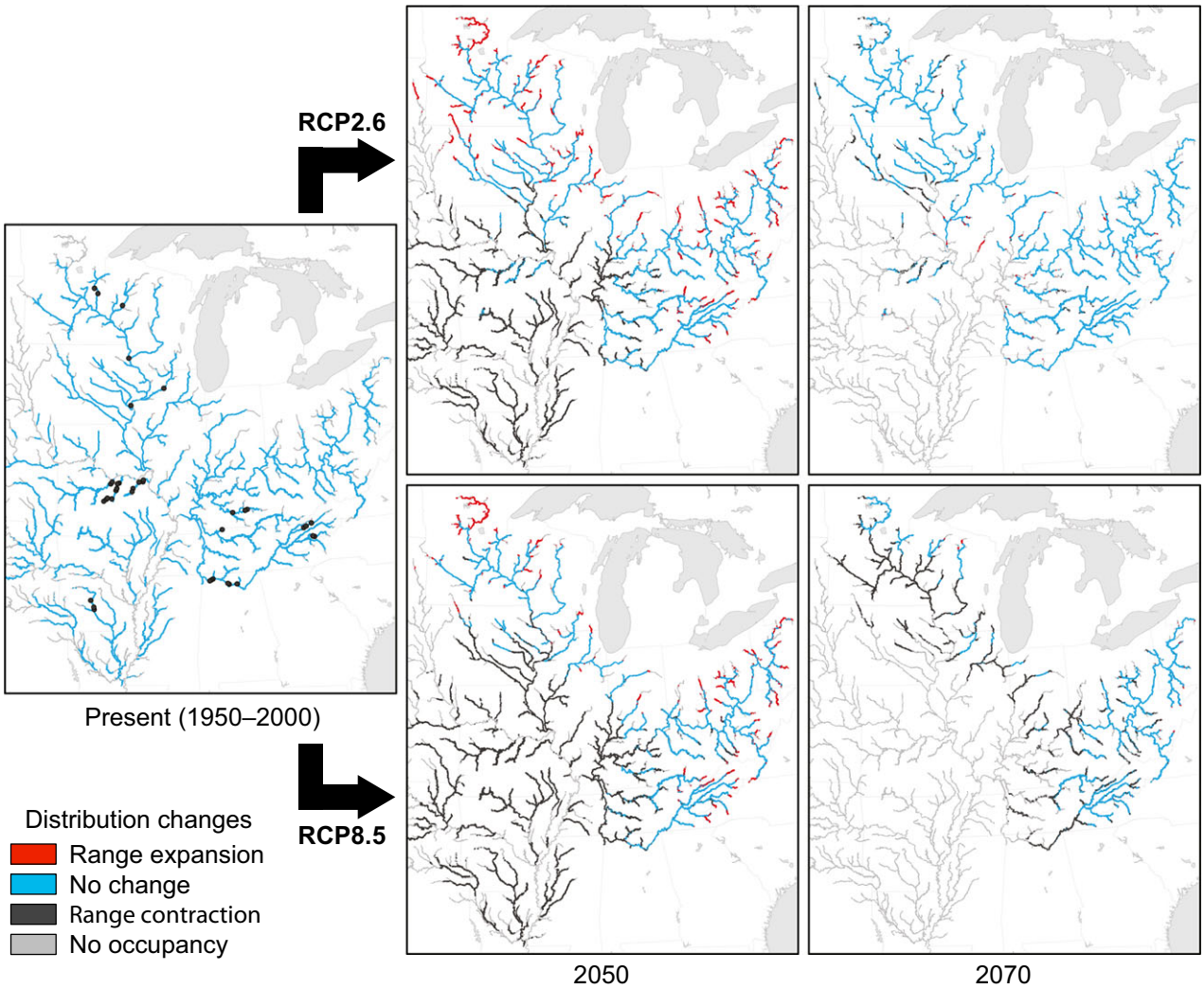

Fig. 3 Maps of predicted suitable (blue) and unsuitable (light gray) habitat for *Cumberlandia monodonta* in the eastern part of the Mississippi River Basin. Suitable habitat was predicted using ecological niche models (ENMs) under 'current' bioclimatic conditions (interpolations of observed data from 1950 to 2000) and hydrological variables, and projections of near-future climate in 2050 (average for 2041–2060) and 2070 (average for 2051–2080). Near-future climate models were under low (upper panels) and high (lower panels) greenhouse gas concentration scenarios (IPCC 5th Assessment). Two representative concentration pathways (RCPs) were used for low and high greenhouse gas concentration scenarios (RCP2.6 and RCP8.5, respectively). Models included ≥ third-order streams of the Mississippi River Basin. Black dots on the Present map represent occurrence points included in the ENMs.

panmixia. Suitable habitat in the Ouachita River was disconnected from the upper Mississippi populations by a long stretch of unsuitable habitat in the lower Mississippi River.

The ENMs for both the RCP2.6 and RCP8.5 scenarios projected range contraction northward and upstream, with drastic declines in suitability scores of the occurrence points throughout the Mississippi River Basin (Figs 3 and S3). In the RCP2.6 scenarios, although suitable habitat expanded toward headwaters in the north and toward higher altitudes, overall suitable habitat declined by 28.7% from the present to 2050, with a further slight decline in habitat from 2050 to 2070 (Table S6; Fig. 3). In 2070, the amount of suitable habitat was 67.2% of the present area of suitable habitat. The average suitability score of the occurrence points declined 38.7% from the present to 2050 (average suitability score = 0.393, SE = 0.035) and remained almost the same in 2070 (average suitability score = 0.370, SE = 0.033). In the RCP8.5 scenarios, on the other hand, suitable habitat declined 48.3% from the current conditions to 2050 and continued to decline from 2050 to 2070 (Table S6; Fig. 3). The average suitability score was 57.7% lower in 2050 (average suitability score = 0.271, SE = 0.033) than at the present and continued to decline through 2070 (average suitability score = 0.167, SE = 0.022).

Projection of the effects of climate change on genetic variation and connectivity

The CDPOP simulations indicated that the magnitude of greenhouse gas concentrations and resultant decrease in stream connectivity due to loss of suitable habitat would alter population connectivity and genetic diversity of the extant populations in the future (Figs 4 and 5). In the no-climate-change model, populations in tributaries of the upper Mississippi River maintained low genetic differentiation and thus remained panmictic (Fig. 4). As a result, genetic diversity remained relatively constant over the simulated period (Fig. 5). The Ouachita populations, on the other hand, were predicted to have slightly increased genetic differentiation while losing ~56% of their total alleles and ~24% of heterozygosity over this time period. Both future climate models predicted loss of panmixia in the upper Mississippi River. In the RCP2.6 model, the Clinch River and St. Croix River populations increased their genetic differentiation versus other populations in the upper Mississippi basin (Fig. 4). Combined with loss of suitable habitat among these populations, these results suggest that climate change under the RCP2.6 scenario would lead to isolation of these populations with significant loss of genetic diversity over time (~72% decrease in total alleles and 27% decrease in heterozygosity over 1000 years; Fig. 5). Furthermore in the RCP8.5 model, the Green River population increased its genetic differentiation versus all other populations (Fig. 4), and accordingly, suffered a drastic reduction in genetic diversity over time (loss of 83% of total alleles and 50% of heterozygosity; Fig. 5). Reduction in the total number of alleles occurred at a much faster rate than did reduction in expected heterozygosity. In both RCP2.6 and RCP8.5 models, populations in the Gasconade, Meramec, and Osage rivers remained panmictic, and maintained relatively stable genetic diversity over time. Regardless of the simulations, among-population variation within rivers remained low (Fig. 4).

Interestingly, these trajectories of population connectivity and genetic diversity over time could not be detected within the first 100 years of simulations (Figs 4 and 5). For example in both climate change scenarios, genetic differentiation among the panmictic populations was subtle at years 2050 and 2100 (Fig. 4); however, differentiation was notable after 300 years of simulations. Similarly, the first 100 years did not show significant reduction in genetic diversity (Fig. 5). In the RCP2.6 model, the Clinch River and St. Croix River populations lost small fractions of the original levels of diversity (17% decrease in total alleles and 1.6% decrease in heterozygosity over 100 years; Fig. 5). Furthermore in the RCP8.5 model, the Green River population showed a 28% reduction in total number of alleles and a 3.2% reduction in heterozygosity over 100 years.

Discussion

Our extensive sampling of *C. monodonta* throughout its range confirmed the existence of a large panmictic population in tributaries of the upper Mississippi River and a genetically isolated population in the Ouachita River, with little or no contemporary gene flow between the Ouachita and other rivers (Inoue *et al.*, 2014). As a result, we consider the Ouachita populations to be an evolutionarily significant unit. Additionally, our study suggests that subtle, but significant, population genetic structure in *C. monodonta* is primarily due to unsuitable habitat in the lower Mississippi River that prevents dispersal between these regions. The presence of panmixia in the upper Mississippi River is made possible by current stream connectivity of highly suitable habitat. Furthermore, the ENMs under current conditions predict potential suitable habitat in headwaters of the Ohio and Mississippi rivers. While these rivers have historic records of *C. monodonta* occurrence (USFWS, 2012), populations within them are thought to be extirpated. The ENMs under future climate scenarios predict that

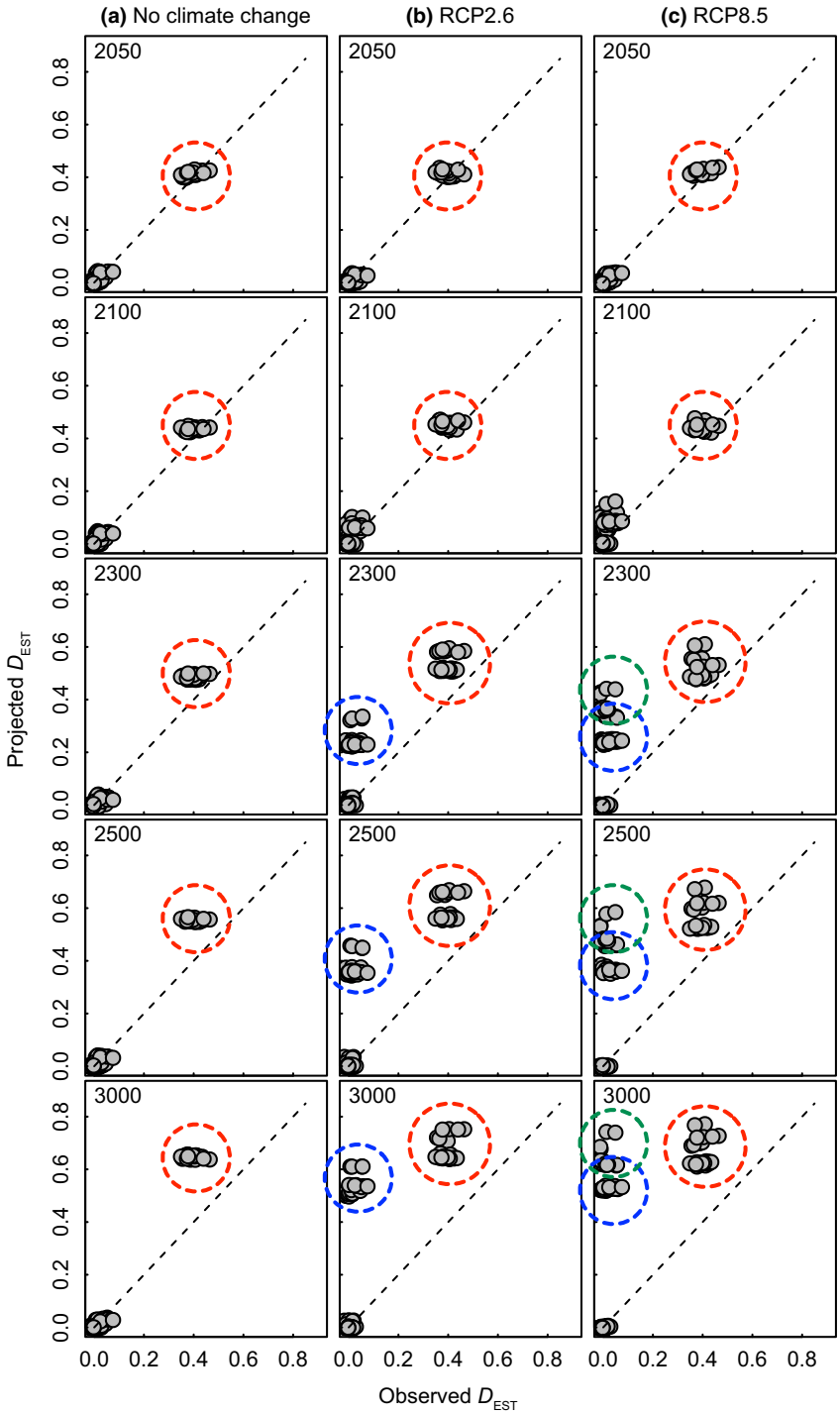

Fig. 4 Results of CDPOP comparing observed (empirical) and projected D_{EST} over 1000 years. Simulations were no-climate-change model (left panels), RCP2.6 model (i.e., low greenhouse gas concentration scenario; middle panels), and RCP8.5 model (i.e., high greenhouse gas concentration scenario; right panel). Dotted lines represent 1:1 relationship. Points above the line indicate that D_{EST} increases in the future (population differentiation increases) and points below the line indicate that D_{EST} decreases in the future. Red circle represents pairwise D_{EST} between OR populations and all other populations; blue circle represents pairwise D_{EST} between CR/SC populations and GR, GRN, MR, and OSG populations; and green circle represents pairwise D_{EST} between GRN population and CR, GR, MR, OSG, and SC populations.

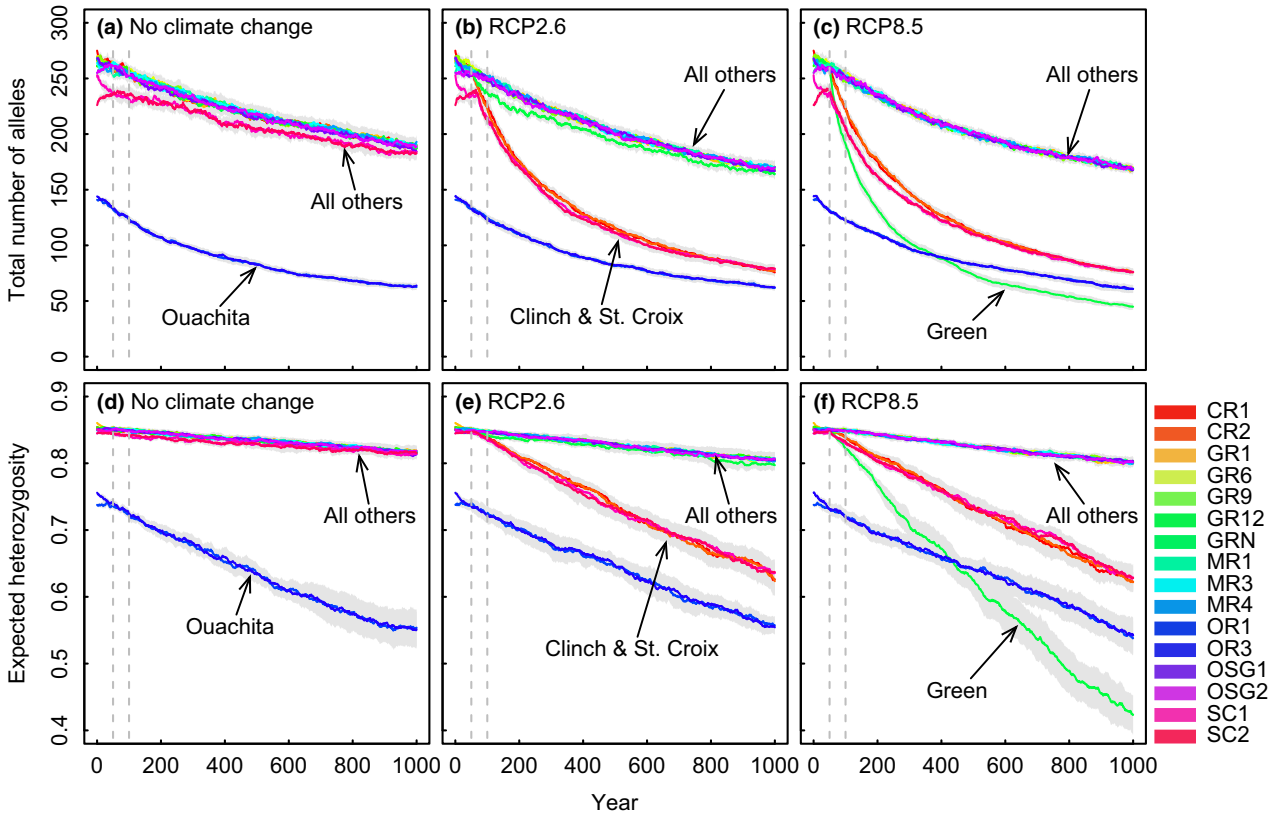

Fig. 5 Results of CDPOP simulations projecting trajectories of genetic diversity (i.e., total number of alleles and expected heterozygosity) over 1000 years under three climate change scenarios. Simulations were based on the no-climate-change model (a and d), the RCP2.6 model (i.e., low greenhouse gas concentration scenario; (b and e), and RCP8.5 model (i.e., high greenhouse gas concentration scenario; (c and f). Vertical lines (dotted gray) represent 50 years and 100 years from present, respectively. Colored lines represent extant populations. Areas of light gray show 95% confidence intervals for each population.

increased greenhouse gas concentration is likely to be correlated with reduction of suitable habitat throughout the Mississippi River Basin, and drastic range contraction northward and upstream. Slight range expansion will occur toward headwaters. In the RCP2.6 scenario, suitable habitat will remain in relatively large portions of the upper Mississippi River, while it will be severely restricted to northern and/or higher altitude headwater tributaries of the Mississippi River in the RCP8.5 scenario. In both scenarios, panmixia in the upper Mississippi River is not likely to be sustained and extant populations will suffer reductions of habitat suitability, especially in populations from the southern portion of the distributional range.

Potential impacts of future climate change on freshwater biodiversity have been reviewed (e.g., Heino *et al.*, 2009), and there is some evidence that freshwater species have exhibited range shifts in response to climate change (e.g., Hickling *et al.*, 2006; Booth *et al.*, 2011). However, these studies typically fail to identify ecological processes (e.g., dispersal, population dynamics) that lead to such range shifts, or consider the genetic consequences of climate change (e.g., changes in gene flow and genetic variability). Our use of ecological and genetic simulations allowed us to explore mechanistic explanations for biological responses to climate change. Although recent population declines of *C. monodonta* are linked to past anthropogenic disturbances other than climate change, in this study we coupled the trajectories of population connectivity and genetic diversity with future effects of climate change. We found that increases in greenhouse gas concentrations are likely to greatly decrease intrapopulation genetic diversity by reducing stream connectivity among populations when we assumed that the current extant populations of *C. monodonta* would remain at the same localities into the future. Our genetic simulations, which accounted for variation in dispersal resistance, showed that fragmentation by long stretches of unsuitable habitat will lead to the loss of panmixia in the upper Mississippi region, resulting in severe declines in genetic diversity. Such outcomes

were very pronounced even in currently well-connected tributaries such as the St. Croix, Clinch, and Green rivers. We note, however, that our genetic trajectories were based upon known populations from seven rivers in the Mississippi River Basin where *C. monodonta* is currently extant. Because our ENMs showed potential suitable habitat in other upper Ohio River and lower Mississippi River drainages, undiscovered populations in such suitable habitat may serve as 'bridges' that have the potential to maintain gene flow between extant populations. For example, relatively large populations were discovered in the Osage and Green rivers in 2012 (USFWS, 2014); several live specimens were found in the Mississippi River near Rock Island, Illinois (T. Smith, personal communication). Similar yet-to-be-discovered populations may help to maintain the current panmictic population in the upper Mississippi River.

The dynamics of range shifts due to warming climates often involve two peripheral edges: the expanding 'leading edge' populations characterized by active colonization events and positive population growth, and contracting 'rear edge' populations that are often small and fragmented such that regional population dynamics cannot easily compensate for local extinction events (Hampe & Petit, 2005). As a result, rear edge populations show reduced genetic diversity within populations and high levels of genetic divergence among populations. Our study suggests that range shifts of *C. monodonta* may involve only the rear edge because expansion of the leading edge toward the pole or to higher altitude is limited by decreases in stream size, as *C. monodonta* generally occurs in large rivers (USFWS, 2014). Given their small size and prolonged isolation (Inoue *et al*., 2014), the current Ouachita River populations display characteristics of rear edge populations. Furthermore, our ENMs predict that mainstems of major drainages (e.g., the upper Mississippi, Ohio, and Tennessee rivers) will lose suitable habitat and thus, suitable habitat in tributaries of these rivers will be fragmented. *Cumberlandia monodonta* and other stream-dwelling species with similar distributions will suffer constriction of ranges at this rear edge. The outcomes of our study allow us to infer the consequences of climate warming for organisms inhabiting other river systems flowing equatorward, including the Colorado River and Rio Grande in the United States, and other great rivers of the world such as the Mekong and Indus. In such systems, species will likely respond to warming climates by shifting their ranges toward the pole or to headwater streams, resulting in isolation of surviving populations due to loss of population connectivity along mainstem reaches.

Given the rate and magnitude with which climate is expected to change in the near future, the link between climate and stream connectivity found in our study has important implications for conservation of *C. monodonta* and other stream-dwelling species in the region. Reducing greenhouse gas emissions may serve to lessen the impacts of climate-change-driven losses in biodiversity and accordingly, prevent local extinctions. Applications of forward-time genetic simulations with ENMs allow prediction of future changes in stream connectivity and the consequences of such changes. We note, however, that there has been much debate about the accuracy of ENM projections when predicting range shifts in response to climate change (Jiménez-Valverde *et al*., 2008; Elith & Leathwick, 2009). Much of the discussion points to the limited ways in which such models consider biological interactions between species and adaptive capacities of individual species (Araújo & Guisan, 2006; de Araújo *et al*., 2014). For example, we developed our ENMs using occurrence records of adult mussels, which may not reflect suitable habitat for host species that carry mussel larvae. A previous study found that ENMs for host species predicted wider distributional ranges of suitable habitats than those of the mussel itself (Inoue *et al*., 2015). Although hosts for *C. monodonta* have not been determined, we expect that such species are likely to be highly mobile and migratory, and have wider ranges of suitable habitats than those of *C. monodonta*. Furthermore, if *C. monodonta* uses multiple host species, each host species might occupy a fraction of the entire range of suitable habitat for *C. monodonta*. If hosts meet such expectations, then surviving *C. monodonta* populations may remain connected via host dispersal as long as distances between such populations are shorter than dispersal distances of individual fish hosts, and fish host ranges continue to overlap with the range of the mussel. Furthermore, warmer trends in climatic regimes can alter physiological and phenological traits to match new climatic conditions (Moran & Alexander, 2014). Although many freshwater organisms may have broad thermal tolerances, warmer temperatures may alter seasonal life cycles and disrupt the timing of reproductive activities. Gametogenesis and glochidia production are triggered by seasonal temperature fluctuations in many mussel species (reviewed in Haag, 2012), including *C. monodonta* (Gordon & Smith, 1990). Because the use of host species varies among mussel species and is often limited to one or a few fishes, changes in the timing of reproductive events may affect biological interactions with host fishes. Particularly, migration and long-distance dispersal of fish are often triggered by seasonal cues, such as water temperature (Ficke *et al*., 2007). These shifts in physiological and phenological traits in

response to climate change may create a mismatch of host–parasite interactions.

Most species tolerate short-term variability in climate through phenotypic plasticity; however, long-term and extreme variability require species to undergo evolutionary changes in order to survive (Jump & Penuelas, 2005). Studies of evolutionary responses to-date, which are limited to invasive species with generation times of 1 year or shorter, show that genetic responses generally develop in a few decades (~25 generations or greater; Moran & Alexander, 2014). However, ongoing climate change is rapid on an evolutionary time scale, especially for species with long generation times; for example, the mean generation time for *C. monodonta* is 26 years (Inoue *et al.*, 2014) and thus, 25 generations is approximately 650 years. Due to a lack of long-term climate projections, our simulations assumed that climatic conditions would be constant after 80 years into the future. We believe that our choices of RCPs represent two 'conservative' climate scenarios, where RCP2.6 assumes that radiative forcing peaks at or before 2100, with constant greenhouse gas emission after 2100 (IPCC, 2013). RCP8.5, on the other hand, assumes that radiative forcing continues to rise until 2250 (IPCC, 2013). Given the relatively poor progress in addressing worldwide emissions of greenhouse gases, it seems likely that any deviations from these scenarios would involve radiative forcing and greenhouse gas emissions that peak even further into the future, which should serve to further increase population discontinuity. Our results suggest that short-term simulations (i.e., ~100 years projections, which are often used for conservation management) would likely fail to detect trajectories of genetic persistence for a species with such long generation times. High levels of overall genetic diversity, large effective population sizes, and high levels of heterozygosity may increase chances of adapting to climate change (Petit & Hampe, 2006), while compensating for decreased individual fitness (Chapman *et al.*, 2009). Thus, high mtDNA and microsatellite diversity would maintain the potential to adapt to rapid climate change for all *C. monodonta* populations except those in the Ouachita River.

We should note that we could not determine whether the genetic signature of panmixia in the upper Mississippi River is due to current gene flow of *C. monodonta* or a legacy of conditions that prevailed prior to modern human impact. We found that short-term simulations failed to show changes in genetic structure. This indicates that even if modern human disturbance fragmented the panmictic population via impoundments, the current population would continue showing characteristics of panmixia for a number of generations. Furthermore, because knowledge of the early life stage of *C. monodonta* is lacking, we used demographic parameters from a relatively well-studied mussel, *Quadrula fragosa*. Future research requires long-term monitoring of the populations and the identification of host species to accurately assess current population structure. Finally, we used neutral markers (i.e., microsatellite loci) to assess genetic diversity and population genetic structure. Because many species exhibit local adaptation to environment and climate (Moran & Alexander, 2014), research to understand the genomic basis of local adaptation will require use of population genomic approaches (e.g., SNPs, RAD-seq; Savolainen *et al.*, 2013).

Global trends in climate change show evidence of poleward range shifts in plant and animal species worldwide (Walther *et al.*, 2002). However, such range shifts are a function of intrinsic dispersal capability and landscape connectivity. While range shifts and changes in landscape connectivity in terrestrial systems are well documented (Hampe & Petit, 2005), less is known about range shifts and habitat connectivity in dendritic systems such as streams. We suggest that riverine systems flowing toward the equator may not exhibit poleward range shifts in biota due to limitations in dispersal ability of aquatic species, loss of connectivity among locations containing suitable habitat, and changes in physical environments due to shifts from larger to smaller streams. Instead, aquatic species inhabiting such systems will be threatened with extirpation unless they are able to adapt to the rapid pace of climate change.

Acknowledgements

We would like to thank M. Davis, B. Sietman, S. McMurray, J. S. Faiman, D. Hubbs, J. Jones, S. Ahlstedt, W. Posey II, J. Harris, C. Lewis, L. Koch, and M. McGregor for help with sampling. Technical assistance was provided by numerous undergraduate technicians in the Berg Lab, and the Center for Bioinformatics and Functional Genomics at Miami University. We thank T. Smith, S. McMurray, J. S. Faiman, T. Crist, B. Cochrane, B. Keane, R. Moore, and several anonymous reviewers for comments on earlier drafts of this manuscript. Funding was provided by the Missouri Department of Conservation and the U.S. Fish and Wildlife Service.

References

Alp M, Keller I, Westram AM, Robinson CT (2012) How river structure and biological traits influence gene flow: a population genetic study of two stream invertebrates with differing dispersal abilities. *Freshwater Biology*, **57**, 969–981.

Altermatt F (2013) Diversity in riverine metacommunities: a network perspective. *Aquatic Ecology*, **47**, 365–377.

Araújo MB, Guisan A (2006) Five (or so) challenges for species distribution modelling. *Journal of Biogeography*, **33**, 1677–1688.

de Araújo CB, Marcondes-Machado LO, Costa GC, Silman M (2014) The importance of biotic interactions in species distribution models: a test of the Eltonian noise hypothesis using parrots. *Journal of Biogeography*, **41**, 513–523.

Baird MS (2000) Life history of the spectaclecase, *Cumberlandia monodonta* Say, 1829 (Bivalvia, Unionoidea, Margaritigeridae). MS Thesis. Southwest Missouri State University, Springfield, Missouri.

Booth DJ, Bond N, Macreadie P (2011) Detecting range shifts among Australian fishes in response to climate change. *Marine and Freshwater Research*, **62**, 1027–1042.

Brown JL (2014) SDMtoolbox: a python-based GIS toolkit for landscape genetic, biogeographic and species distribution model analyses. *Methods in Ecology and Evolution*, **5**, 694–700.

Butler RS (2002) *Status Assessment Report for the Spectaclecase, Cumberlandia monodonta, Occurring in the Mississippi River System (U.S. Fish and Wildlife Service Regions 3, 4, 5, and 6).* pp. 69, The Ohio River Valley Ecosystem Team, Asheville, NC.

Campbell Grant EH, Lowe WH, Fagan WF (2007) Living in the branches: population dynamics and ecological processes in dendritic networks. *Ecology Letters*, **10**, 165–175.

Chapman JR, Nakagawa S, Coltman DW, Slate J, Sheldon BC (2009) A quantitative review of heterozygosity-fitness correlations in animal populations. *Molecular Ecology*, **18**, 2746–2765.

Chen I-C, Hill JK, Ohlemüller R, Roy DB, Thomas CD (2011) Rapid range shifts of species associated with high levels of climate warming. *Science*, **333**, 1024–1026.

Dudgeon D, Arthington AH, Gessner MO *et al.* (2006) Freshwater biodiversity: importance, threats, status and conservation challenges. *Biological Reviews*, **81**, 163–182.

Earl DA, vonHoldt BM (2012) STRUCTURE HARVESTER: a website and program for visualizing STRUCTURE output and implementing the Evanno method. *Conservation Genetics Resources*, **4**, 359–361.

Elith J, Leathwick JR (2009) Species distribution models: ecological explanation and prediction across space and time. *Annual Review of Ecology, Evolution, and Systematics*, **40**, 677–697.

Elith J, Phillips SJ, Hastie T, Dudík M, Chee YE, Yates CJ (2011) A statistical explanation of MaxEnt for ecologists. *Diversity and Distributions*, **17**, 43–57.

Etherington TR (2011) Python based GIS tools for landscape genetics: visualising genetic relatedness and measuring landscape connectivity. *Methods in Ecology and Evolution*, **2**, 52–55.

Fagan WF (2002) Connectivity, fragmentation, and extinction risk in dendritic metapopulations. *Ecology*, **83**, 3243–3249.

Felsenstein J (2005) *PHYLIP (Phylogeny Inference Package) Version 3.6*. Department of Genome Sciences, University of Washington, Seattle, WA.

Ficke AD, Myrick CA, Hansen LJ (2007) Potential impacts of global climate change on freshwater fisheries. *Reviews in Fish Biology and Fisheries*, **17**, 581–613.

Geffen E, Anderson MJ, Wayne RK (2004) Climate and habitat barriers to dispersal in the highly mobile grey wolf. *Molecular Ecology*, **13**, 2481–2490.

Gerlach G, Jueterbock A, Kraemer P, Deppermann J, Harmand P (2010) Calculations of population differentiation based on G_{ST} and D: forget G_{ST} but not all of statistics!. *Molecular Ecology*, **19**, 3845–3852.

Gordon ME, Smith DG (1990) Autumnal reproduction in *Cumberlandia monodonta* (Unionoidea: Margaritiferidae). *Transactions of the American Microscopical Society*, **109**, 407–411.

Goudet J (2005) HIERFSTAT, a package for R to compute and test hierarchical *F*-statistics. *Molecular Ecology Notes*, **5**, 184–186.

Haag WR (2009) A hierarchical classification of freshwater mussel diversity in North America. *Journal of Biogeography*, **37**, 12–26.

Haag WR (2012) *North American Freshwater Mussels: Natural History, Ecology, and Conservation*. Cambridge University Press, Cambridge, UK.

Habel JC, Rödder D, Schmitt T, Nève G (2011) Global warming will affect the genetic diversity and uniqueness of *Lycaena helle* populations. *Global Change Biology*, **17**, 194–205.

Hall LA, Beissinger SR (2014) A practical toolbox for design and analysis of landscape genetics studies. *Landscape Ecology*, **29**, 1487–1504.

Hampe A, Petit RJ (2005) Conserving biodiversity under climate change: the rear edge matters. *Ecology Letters*, **8**, 461–467.

Heino J, Virkkala R, Toivonen H (2009) Climate change and freshwater biodiversity: detected patterns, future trends and adaptations in northern regions. *Biological Reviews*, **84**, 39–54.

Hickling R, Roy DB, Hill JK, Fox R, Thomas CD (2006) The distributions of a wide range of taxonomic groups are expanding polewards. *Global Change Biology*, **12**, 450–455.

Hijmans RJ, Cameron SE, Parra JL, Jones PG, Jarvis A (2005) Very high resolution interpolated climate surfaces for global land areas. *International Journal of Climatology*, **25**, 1965–1978.

Hughes JM, Schmidt DJ, Finn DS (2009) Genes in streams: using DNA to understand the movement of freshwater fauna and their riverine habitat. *BioScience*, **59**, 573–583.

Inoue K, Moyer GR, Williams A, Monroe EM, Berg DJ (2011) Isolation and characterization of 17 polymorphic microsatellite loci in the spectaclecase, *Cumberlandia monodonta* (Bivalvia: Margaritiferidae). *Conservation Genetics Resources*, **3**, 57–60.

Inoue K, Monroe EM, Elderkin CL, Berg DJ (2014) Phylogeographic and population genetic analyses reveal Pleistocene isolation followed by high gene flow in a wide-ranging, but endangered, freshwater mussel. *Heredity*, **112**, 282–290.

Inoue K, Lang BK, Berg DJ (2015) Past climate change drives current genetic structure of an endangered freshwater mussel species. *Molecular Ecology*, **24**, 1910–1926.

IPCC (2013) Summary for policymakers. In: *Climate Change 2013: The Physical Science Basis. Contribution of Working Group I to the Fifth Assessment Report of the Intergovernmental Panel on Climate Change* (eds Stocker TF, Qin D, Plattner G-K, Tignor M, Allen SK, Boschung J, Nauels A, Xia Y, Bex V, Midgley PM), pp. 3–29. Cambridge University Press, Cambridge, UK.

Jakobsson M, Rosenberg NA (2007) CLUMPP: a cluster matching and permutation program for dealing with label switching and multimodality in analysis of population structure. *Bioinformatics*, **23**, 1801–1806.

Jiménez-Valverde A, Lobo JM, Hortal J (2008) Not as good as they seem: the importance of concepts in species distribution modelling. *Diversity and Distributions*, **14**, 885–890.

Jost L (2008) G_{ST} and its relatives do not measure differentiation. *Molecular Ecology*, **17**, 4015–4026.

Jump AS, Penuelas J (2005) Running to stand still: adaptation and the response of plants to rapid climate change. *Ecology Letters*, **8**, 1010–1020.

Kjos C, Byers O, Miller P, Borovansky J, Seal US (1998) *Population and Habitat Viability Assessment Workshop for the Winged Mapleleaf Mussel (Quadrula fragosa): Final Report*. pp. 92, CBSG, Apple Valley, Minnesota.

Kramer-Schadt S, Niedballa J, Pilgrim JD *et al.* (2013) The importance of correcting for sampling bias in MaxEnt species distribution models. *Diversity and Distributions*, **19**, 1366–1379.

Landguth EL, Cushman SA (2010) CDPOP: a spatially explicit cost distance population genetics program. *Molecular Ecology Resources*, **10**, 156–161.

Landguth EL, Schwartz MK (2014) Evaluating sample allocation and effort in detecting population differentiation for discrete and continuously distributed individuals. *Conservation Genetics*, **15**, 981–992.

Librado P, Rozas J (2009) DnaSP v5: a software for comprehensive analysis of DNA polymorphism data. *Bioinformatics*, **25**, 1451–1452.

Moran EV, Alexander JM (2014) Evolutionary responses to global change: lessons from invasive species. *Ecology Letters*, **17**, 637–649.

Parmesan C, Yohe G (2003) A globally coherent fingerprint of climate change impacts across natural systems. *Nature*, **421**, 37–42.

Peakall R, Smouse PE (2006) GENALEX 6: genetic analysis in Excel. Population genetic software for teaching and research. *Molecular Ecology Notes*, **6**, 288–295.

Pearson RG, Raxworthy CJ, Nakamura M, Peterson AT (2007) Predicting species distributions from small numbers of occurrence records: a test case using cryptic geckos in Madagascar. *Journal of Biogeography*, **34**, 102–117.

Peterson EE, Ver Hoef JM, Isaak DJ *et al.* (2013) Modelling dendritic ecological networks in space: an integrated network perspective. *Ecology Letters*, **16**, 707–719.

Petit RJ, Hampe A (2006) Some evolutionary consequences of being a tree. *Annual Review of Ecology, Evolution, and Systematics*, **37**, 187–214.

Phillips SJ, Anderson RP, Schapire RE (2006) Maximum entropy modeling of species geographic distributions. *Ecological Modelling*, **190**, 231–259.

Phillips SJ, Dudik M, Elith J, Graham CH, Lehmann A, Leathwick JR, Ferrier S (2009) Sample selection bias and presence-only distribution models: implications for background and pseudo-absence data. *Ecological Applications*, **19**, 181–197.

Pritchard JK, Stephens M, Donnelly P (2000) Inference of population structure using multilocus genotype data. *Genetics*, **155**, 945–959.

R Core Team (2015) *R: A Language and Environment for Statistical Computing*. R Foundation for Statistical Computing, Vienna, Austria. https://www.r-project.org.

Rosenberg NA (2004) DISTRUCT: a program for the graphical display of population structure. *Molecular Ecology Notes*, **4**, 137–138.

Rousset F (2008) GENEPOP'007: a complete re-implementation of the GENEPOP software for Windows and Linux. *Molecular Ecology Resources*, **8**, 103–106.

Row JR, Wilson PJ, Gomez C, Koen EL, Bowman J, Thornton D, Murray DL (2014) The subtle role of climate change on population genetic structure in Canada lynx. *Global Change Biology*, **20**, 2076–2086.

Savolainen O, Lascoux M, Merila J (2013) Ecological genomics of local adaptation. *Nature Reviews Genetics*, **14**, 807–820.

Sexton JP, Hangartner SB, Hoffmann AA (2014) Genetic isolation by environment or distance: which pattern of gene flow is most common? *Evolution*, **68**, 1–15.

Szpiech ZA, Jakobsson M, Rosenberg NA (2008) ADZE: a rarefaction approach for counting alleles private to combinations of populations. *Bioinformatics*, **24**, 2498–2504.
Urban D, Keitt T (2001) Landscape connectivity: a graph-theoretic perspective. *Ecology*, **82**, 1205–1218.
US Fish and Wildlife Service (USFWS) (2012) Endangered and threatened wildlife and plants; determination of endangered status for the sheepnose and spectaclecase mussels throughout their range, final rule. *Federal Register*, **77**, 14914–14949.
U.S. Fish and Wildlife Service (USFWS) (2014) *Recovery Outline for the Spectaclecase mussel (Cumberlandia monodonta) – January 2014*. US Fish and Wildlife Service, Fort Snelling, MN.
Vörösmarty CJ, McIntyre PB, Gessner MO *et al*. (2010) Global threats to human water security and river biodiversity. *Nature*, **467**, 555–561.
Walther GR, Post E, Convey P *et al*. (2002) Ecological responses to recent climate change. *Nature*, **416**, 389–395.

Supporting Information

Additional Supporting Information may be found in the online version of this article:

Table S1. Descriptive statistics for COI sequences and 16 microsatellite loci for each collection site of *Cumberlandia monodonta*.
Table S2. Museum records and field surveys of *Cumberlandia monodonta* used in ecological niche modeling (ENM).
Table S3. Bioclimatic, geographic, and landscape layers used in ecological niche models.
Table S4. Results of the hierarchical analysis of molecular variance (AMOVA) in *Cumberlandia monodonta*.
Table S5. Pairwise D_{EST} (above diagonal) and F_{ST} (below diagonal) values for 16 microsatellite loci from 17 populations of *Cumberlandia monodonta*.
Table S6. Areas (km^2) of binary predictions of suitable and unsuitable habitat under current conditions and two greenhouse gas concentration scenarios in 2050 and 2070.
Figure S1. A parsimony network of COI sequences for *Cumberlandia monodonta*.
Figure S2. (a) Log-likelihood [Ln P(k)] and (b) Δk for each k over the 10 replicates in STRUCTURE.
Figure S3. Potential suitable habitat for *Cumberlandia monodonta* identified by ecological niche models (ENMs) using both 'current' bioclimatic conditions and landscape variables, and projections of four near-future climate scenarios.